Quantitative definition of patterns in soft-mode turbulence suppressing the Nambu-Goldstone mode

Fahrudin Nugroho,[1,2,*] Tatsuhiro Ueki,[1] Rinto Anugraha,[1,2] Yoshiki Hidaka,[1] and Shoichi Kai[1]

[1]*Department of Applied Quantum Physics and Nuclear Engineering, Graduate School of Engineering, Kyushu University, Fukuoka 819-0395, Japan*

[2]*Department of Physics, Faculty of Mathematics and Natural Sciences, Gadjah Mada University, Bulaksumur BLS 21, Yogyakarta 55281, Indonesia*

(Received 23 February 2011; revised manuscript received 18 May 2011; published 28 July 2011)

Chaotic patterns in electroconvection of homeotropic nematics, soft-mode turbulence (SMT), and the related spatiotemporal chaos (STC) are discussed, and the quantitative definition of the patterns is considered. The order parameter S, obtained directly from the 2D spectra of the patterns, is introduced. The contribution of the Nambu-Goldstone mode and the increase in pattern regularity under the influence of an external magnetic field $\mathbf{H}$ are evaluated. We propose a schematic phase diagram of STC patterns based on the value of S.

DOI: 10.1103/PhysRevE.84.011709 PACS number(s): 61.30.−v, 05.45.−a, 82.40.Bj, 89.75.Kd

I. INTRODUCTION

Numerous patterns can be observed in nonlinear systems far from equilibrium, and have attracted the attention of many researchers. They frequently show chaotic behavior [1], especially when regularity is broken and replaced by disorder state. Rayleigh-Bénard convection is a standard example of such systems, and produces several complex patterns including chaos and turbulence with variations of the control parameter [2]. In order to properly classify them, quantitative definitions of regularity and complexity become important [3].

One new example of the above mentioned systems is ac-driven electroconvection in a nematic liquid crystal. This system shows very rich spatial and temporal disordered patterns [4–7], and supplies a wide range of opportunities for the quantitative definition of such patterns and of chaos. Moreover, this system has two big advantages: well controlled external fields and initial symmetry [8]. By controlling the electric and/or magnetic fields, the chaoticity of the pattern can be adjusted qualitatively. In addition, there are two realizations of these systems, planar and homeotropic nematics, which are related to translational and rotational initial symmetry. Here we focus on pattern formation in homeotropic nematics because they exhibit various nontrivial chaotic patterns.

In the homeotropic system, treating the electrodes with a surfactant such as N,N-dimethyl-N-octadecyl-3-aminopropyltrimethoxysilyl-chloride (DMOAP) can align the average orientation of the nematic, the director $\mathbf{n}$, perpendicular to the confining surfaces. Therefore there exists continuous rotational symmetry on a plane parallel to the electrodes (the x-y plane). Due to negative dielectric anisotropy of the material, there is a threshold of applied voltage $V_{\rm ac}(t) = \sqrt{2}V\cos(2\pi f t)$, called Fréedericksz threshold $V_{\rm F}$ (=3.5 V), above which $\mathbf{n}$ tilts with respect to the z axis, and the rotational invariance in the x-y plane is broken. Since the two-dimensional director $\mathbf{c}(\mathbf{r})$, where $\mathbf{r} = (x,y)$, which is the projection of $\mathbf{n}$ onto the x-y plane, can freely rotate in this plane [9–11], the azimuthal rotation of the tilted director behaves as a Nambu-Goldstone mode. After increasing V beyond the convection threshold $V_{\rm c}$, electroconvection occurs with local wave vector $\mathbf{q}(\mathbf{r})$. The electroconvection interacts with the $\mathbf{c}(\mathbf{r})$ director [8]. This interaction induces unstable states and yields a new type of spatiotemporal chaos (STC) called soft-mode turbulence (SMT) [12,13]. With respect to the ac frequency f of the applied voltage, there are two types of SMT patterns in the oblique roll (OR) and normal roll (NR) regimes [14] in which the corresponding ac frequency is below and beyond the Lifshitz frequency $f_{\rm L}$, respectively [15,16]. Additionally, by applying an external magnetic field $\mathbf{H} = (H,0,0)$ the behavior of the pattern is changed, since the application of $\mathbf{H}$ suppresses the Nambu-Goldstone mode [17].

Several articles have considered the effects of applying $\mathbf{H}$ to electroconvective patterns [11,15,18–22]. The stabilization of patterns owing to $\mathbf{H}$ in the NR regime as well as the corresponding destabilization via creation of dislocations has been reported and compared with the theory [18]. While at the OR regime, Huh *et al.* [15,21] observed the H dependence of the patterns and discovered two types of disordered patterns which are qualitatively different observed at two different fixed values of H that are 400 [G] and 1000 [G]. These were referred to as a spatially isotropic pattern (STC A) and a spatially anisotropic pattern (STC B), respectively. However, the difference and the boundary between the patterns, especially in the OR regime, are unclear.

In the present paper we introduce an improved order parameter to understand such changes in SMT patterns affected by suppression of the Nambu-Goldstone mode. Using this order parameter, we make a quantitative definition of the pattern structures including STC A and STC B. Finally, we applied the order parameter to construct a schematic phase diagram of patterns describing variety of routes of changes in the pattern. The present research can provide quantitative criteria of pattern regularity and enable the classification of electroconvective patterns types.

II. EXPERIMENT AND DISCUSSION

We performed an experiment using a nematic liquid crystal N-(4-methoxybenzylidene)-4-butylaniline (MBBA)

*fahrudin@athena.ap.kyushu-u.ac.jp

sandwiched between two glass plates with the distance $d = 52 \pm 1\ \mu$m. The setup was similar to that described in a previous paper [23]. Circular electrodes of indium tin oxide (ITO) with a diameter of 12.9 mm were coated on the glass plates. The measurements were conducted at a stabilized temperature of $30.00 \pm 0.05\ ^\circ$C. The dielectric constant $\epsilon_{||}$ and the electric conductivity $\sigma_{||}$ of the sample cell were 6.4 ± 0.1 and $8.7 \pm 0.1 \times 10^{-7}\ \Omega^{-1}\ \mathrm{m}^{-1}$, respectively. A constant H, applied collateral to the electrodes, was generated from an electromagnet (TAMAGAWA GP060-60R), and the strength was measured by a Gauss meter (Yokogawa 3251). A CCD camera (Sony XCL 5005) was mounted on a microscope, and software (DPX-CLM 100 basic) was used to capture pattern images in the x-y plane. The size of the images was 1.14 mm $\times$ 1.14 mm (1000 pixels $\times$ 1000 pixels).

The following procedure was used to obtain the images. First, we defined a control parameter $\varepsilon \equiv (V/V_c)^2 - 1$. Note that in the previous publications [18,22] an effect of ordering in SMT patterns due to variation of frequency f of applied voltage was reported. Therefore, to avoid the change in SMT pattern due to shift of the Lifshitz frequency f_L by varying H, we used a fixed normalized frequency of $\eta \equiv \frac{f - f_L(H)}{f_L(H)} = -0.5$, which corresponds to the oblique rolls (OR) regime [8]. We applied a constant H below the Fréedericksz threshold H_F (=1050 G) and waited for 1 min. Then we increased V above V_F and waited 10 min until a homogenous state of $\mathbf{c}(\mathbf{r})$ director was reached. Then we raised V above V_c to obtain a desired value of ε, and waited 20 min for any transient state to pass. Images were captured at intervals of 2 min. Image analysis was performed by ImageJ and customized software.

The typical convective patterns at fixed $\varepsilon = 0.2$ and $\eta = -0.5$ for various H are shown in Figs. 1(a)–1(d), while Figs. 1(e)–1(h) show the corresponding 2D spectra. We observed an increase in the degree of regularity of the convective patterns with increasing H [see Figs. 1(a)–1(d)]. The corresponding 2D spectra [Figs. 1(e)–1(h)] changed from a uniform ring to a more heterogeneous one, and focused into a narrow region near the q_x axis in the direction of $\mathbf{H}$. To observe the change in the homogeneity of the spectrum increasing in H, we plotted the intensity I of the spectrum as a function of the azimuthal angle ϕ (as shown in Fig. 2). The intensity profiles became higher and sharper, indicating $\mathbf{q}(\mathbf{r})$ oriented along a single preferred direction as H increased; that is, a more ordered pattern was observed. According to the naming by Huh *et al.*, the patterns shown in Fig. 1(a) [corresponding to Fig. 1(e)] is called STC A, and those of Figs. 1(b) and 1(c) [corresponding to Figs. 1(f) and 1(g)] are called STC B, while Fig. 1(d) [corresponding to Fig. 1(h)] is an ordered pattern, but no comprehensive quantitative definition was done. Therefore, we attempted it as follows.

We define an improved order parameter S indicating the pattern regularity based on the intensity modulation in the ring of the 2D spectra, as follows:

$$S = \frac{\int_{-\pi/2}^{\pi/2} [I(\phi) - I_{\min}] d\phi}{\int_{-\pi/2}^{\pi/2} [I(\phi)] d\phi}, \qquad (1)$$

where I and $I_{\min}$ are the intensity of the spectrum as a function of ϕ and its minimum value, respectively. Qualitatively, S may be described as the comparison of the power spectral of the

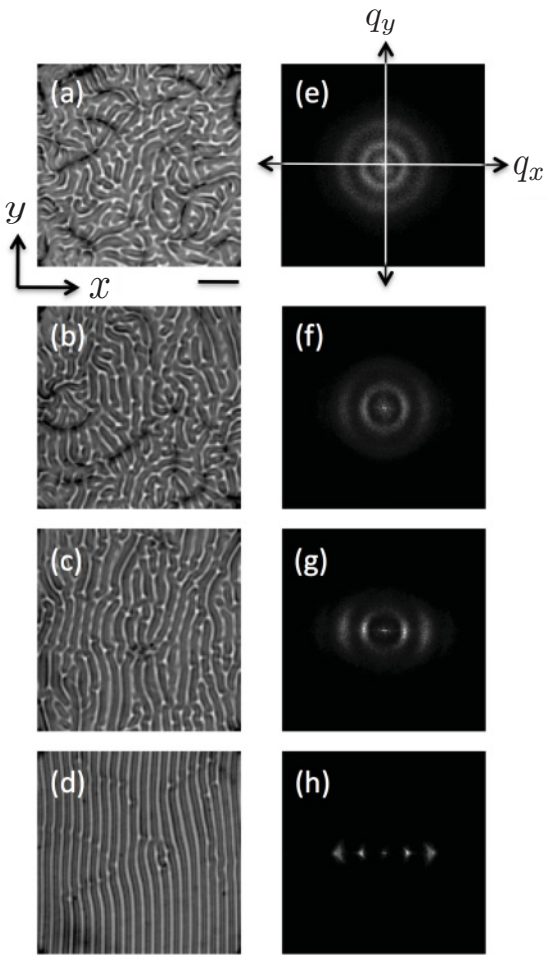

FIG. 1. The decrease in complexity of the convective patterns under the influence of H for (a) $H = 50$ G, (b) $H = 350$ G, (c) $H = 450$ G, and (d) $H = 650$ G for a fixed $\varepsilon = 0.2$. The corresponding 2D spectra are shown in (e), (f), (g), and (h), respectively. The length of the bar is 200 μm. The image contrast was enhanced, so that the rolls and low intensity spectra are easier to see.

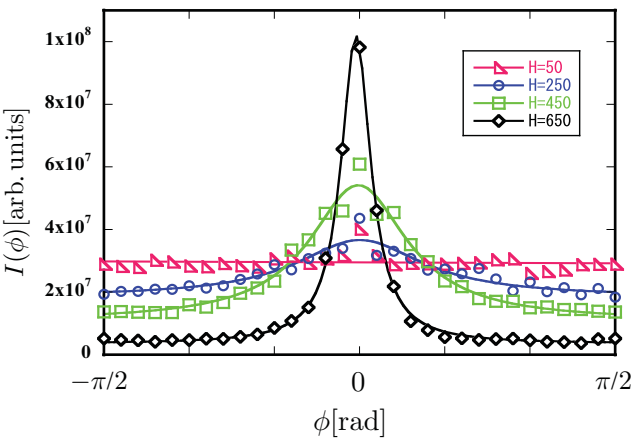

FIG. 2. (Color online) The intensity I of the first-mode spectrum vs azimuthal angle ϕ for various values of H at fixed $\varepsilon = 0.2$. Solid lines indicate the Lorenzian functions.

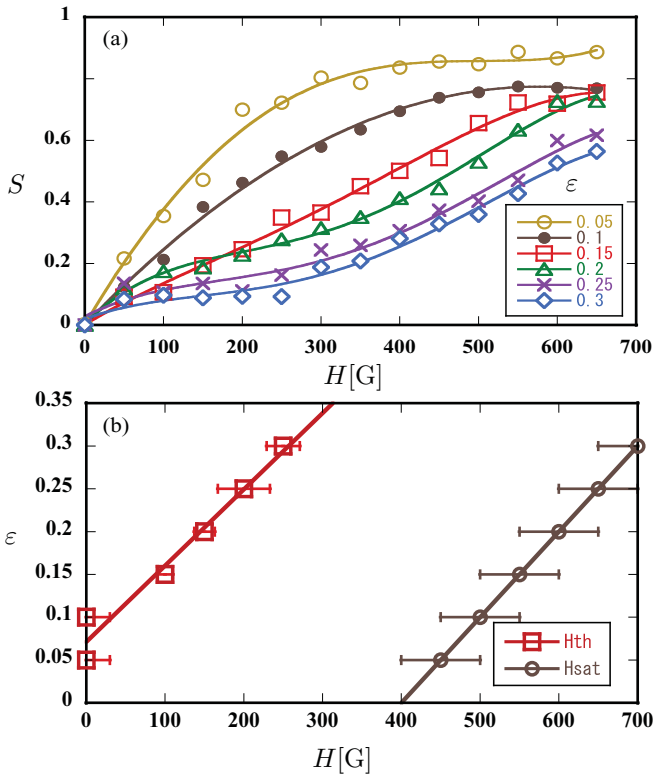

FIG. 3. (Color online) (a) Magnetic field H dependence of the order parameter S. For higher ε, the value of S increased more gradually, since the original pattern ($H = 0$) was more chaotic. The lines were added as a visual guide. (b) The threshold field $H_{\rm th}$ at which the value of S linearly increased (red rectangles), and the saturated field $H_{\rm sat}$ indicates that S began to saturate (brown circles). See text for details.

signal response to its total power, including the background. The approach used here is sufficient to characterize the changes in orientation of $\mathbf{q}(\mathbf{r})$ regarding both the amplitudes and the widths of the 2D spectra. The H dependence of S for various values of ε are shown in Fig. 3.

Figure 3 shows that S increased from zero with increasing H, and finally saturated at sufficient H. For $\varepsilon < 0.15$ the value of S immediately increase even for small H showing an exponential type against H. However, for $\varepsilon \geqslant 0.15$ the value of S becomes constant after small increase at small H. Since then with increases H, S sharply increases similar a shape of logistic curve type with a plateau regime in the middle (actually not fit well to logistic equations). Thus, a clear shape change of S-H curves is observed at some H (hereafter called $H_{\rm th}$). Therefore we introduce for convenience two distinguishable fields $H_{\rm th}$ above which S sharply increases and $H_{\rm sat}$ is defined by H at which S starts to saturate. In Fig. 3 we observed there were two different profiles of S, namely a convex and a concave versus H for $\varepsilon < 0.15$ and $\varepsilon \geqslant 0.15$, respectively. From the presence of such different S profiles, two important conclusions can be drawn.

First, for $\varepsilon \geqslant 0.15$, the fluctuations of $\mathbf{c}(\mathbf{r})$ and $\mathbf{q}(\mathbf{r})$ were considerably robust. After applying $H \leqslant H_{\rm th}$, $\mathbf{c}(\mathbf{r})$ could no longer freely rotate, because the symmetry of $\mathbf{c}(\mathbf{r})$ was broken by the application of $\mathbf{H}$. However, $\mathbf{q}(\mathbf{r})$ still freely rotates because of the uncompensated torque [8,17,20]. Further evidence can be seen in the flat profile of $I(\phi)$ in Fig. 2 for $H = 50$ G, which indicates that all directions of $\mathbf{q}(\mathbf{r})$ remained possible. The pattern therefore remained similar to the SMT [see Fig. 1(a)], and was now called STC A [21]. Here the values of S have a concave-type increment, for example, plateau-like at constant $S \approx 0.1$ indicating the influence of the Nambu-Goldstone mode for $H \leqslant H_{\rm th}$ (STC A). Then, S monotonically increased with increasing $H > H_{\rm th}$, because $\mathbf{q}(\mathbf{r})$ no longer freely rotates. The regularity of the convective pattern increased, and was called STC B [see Fig. 1(c)] [21]. Therefore, as shown in Fig. 3(a), $H_{\rm th}$ is the threshold field between STC A [formed by free rotation of $\mathbf{q}(\mathbf{r})$] and STC B [$\mathbf{q}(\mathbf{r})$ no longer freely rotates].

Second, for $\varepsilon < 0.15$, both $\mathbf{c}(\mathbf{r})$ and $\mathbf{q}(\mathbf{r})$ infirmly fluctuate. With the application of $\mathbf{H}$, free rotation of $\mathbf{c}(\mathbf{r})$ is sufficiently suppressed, and $\mathbf{c}(\mathbf{r})$ no longer behaved as the Nambu-Goldstone mode. $\mathbf{q}(\mathbf{r})$ also no longer freely rotates. As a result, the pattern drastically changed from isotropic to more regular; that is, STC B [21]. The corresponding spectrum in Fig. 2 changed from a flat profile to a narrow peak. Consequently, the value of S steeply increased, forming a convex profile.

These results can be explained as follows. For small ε (slightly above the onset $\varepsilon = 0$), the patterns are produced by flow induced by electroconvection. Such flow involves weak chaos (slow dynamics of irregular motions in convection), and the application of H easily leads to more regular patterns. On the other hand, for larger ε, the flow becomes stronger and induces faster and more irregular motions. In that case, a strong H is necessary to obtain more regular patterns.

Furthermore, increasing H above the saturated field $H_{\rm sat}$, the values of S for both $\varepsilon < 0.15$ and $\varepsilon \geqslant 0.15$ become saturated. The $H_{\rm sat}$ values are given in Fig. 3(a). In this regime, the convective pattern is periodic [see Fig. 1(d)] because the rotational freedoms of $\mathbf{c}(\mathbf{r})$ as well as $\mathbf{q}(\mathbf{r})$ are almost fully suppressed. The local wave vector $\mathbf{q}(\mathbf{r})$, however, slightly fluctuates in the $\mathbf{H}$ direction for finite ε.

In order to obtain more information on the pattern structure in the saturated regime of S, specifically $\varepsilon = 0.05$ with $H = 500$ G, we employed crossed polarizer observations. As shown in Figs. 4(a) and 4(b), we observed the coexistence of

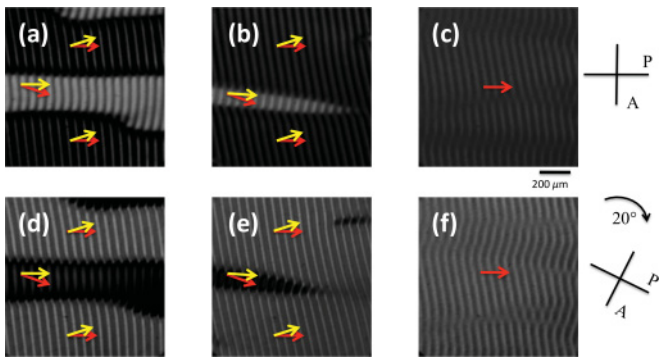

FIG. 4. (Color online) Typical patterns obtained from crossed polarizer observation with $\varepsilon = 0.05$ and a fixed $\eta = -0.5$ under the influence of $H = 500$, 550, and 600 G in (a), (b), and (c), respectively. (d), (e), and (f) are the corresponding images after rotating the crossed polarizer 20 deg clockwise. The red (dark) and yellow (bright) arrows indicate the directions of $\mathbf{c}(\mathbf{r})$ and $\mathbf{q}(\mathbf{r})$, respectively.

zig and zag formations; that is, an abnormal zigzag pattern (Z-II) was formed [5]. The zig (zag) domain corresponds to the dark (bright) areas in Fig. 4(a), in which the $\mathbf{c}(\mathbf{r})$ director was parallel (not parallel) with one of the polarizers. A 20 deg azimuthal angle of $\mathbf{c}(\mathbf{r})$ between a zig and a zag domain was obtained by rotating the crossed polarizer (see Fig. 4). After increasing H to $H = 550$ G, the zag area decreased. Finally, the abnormal zigzag formation was eliminated at higher H (600 G) for $\varepsilon = 0.05$. The orientation of $\mathbf{c}(\mathbf{r})$ in the x-y plane became uniform, leaving a normal zigzag (Z-I) pattern [see Figs. 4(c) and 4(d)] [5]. It is an evident that in the saturated regime there was a pattern transition from abnormal zigzag pattern (Z-II) to normal zigzag ones (Z-I).

Based on S, we can categorize the electroconvective patterns and the degree of regularity under a symmetry breaking caused by H, as follows:

(i) An original SMT pattern ($H = 0$) is indicated by $S = 0$.

(ii) STC A ($H \leqslant H_{\rm th}$) exists in the regime corresponding to $0 < S \leqslant 0.1$ including the plateau region at $S \approx 0.1$ in the present study. Such a plateau indicates an occurrence of STC A. In this regime, $\mathbf{q}(\mathbf{r})$ can still freely rotate. The pattern is therefore chaotic and isotropic like SMT.

(iii) STC B ($H > H_{\rm th}$) exists in the regime corresponding to $S > 0.1$, and S linearly increases with increasing in H. Both $\mathbf{c}(\mathbf{r})$ and $\mathbf{q}(\mathbf{r})$ in this regime are no longer free to rotate. Therefore, more ordered patterns were observed.

(iv) The transition from an abnormal zigzag pattern (Z-II) to a normal zigzag pattern (Z-I) ($H \geqslant H_{\rm sat}$) occurs in the regime with saturated S. Both an abnormal zigzag pattern (Z-II) and a normal zigzag pattern (Z-I) are almost ordered patterns ($S \geqslant 0.8$). Crossed polarizer observation is necessary to distinguish them.

The schematic phase diagram of patterns in the H-ε plane is shown in Fig. 5.

Using S, as defined in Eq. (1), the relative degree of order showing regularity, that is, deviation from the chaotic state, can be measured quantitatively [24]. Thus, S can serve as a new measure of pattern regularity in SMT. The value of S is bounded as $0 \leqslant S \leqslant 1$, and with $S = 0$ (or $S = 1$) the pattern corresponds to that of SMT (or a completely striped one). Therefore, the value of S is also related to how much

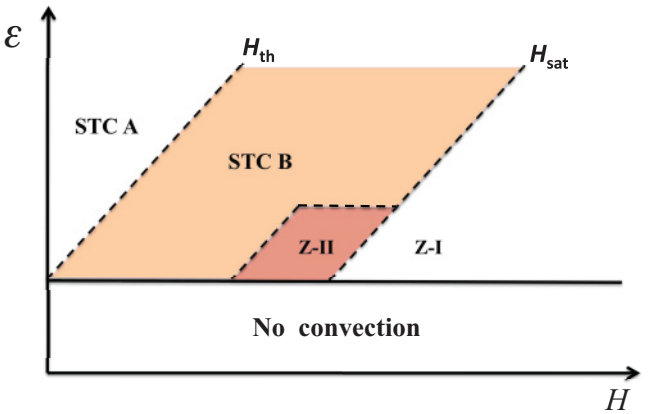

FIG. 5. (Color online) The schematic phase diagram of the patterns in the H-ε plane. The type of patterns can be defined based on the values of S.

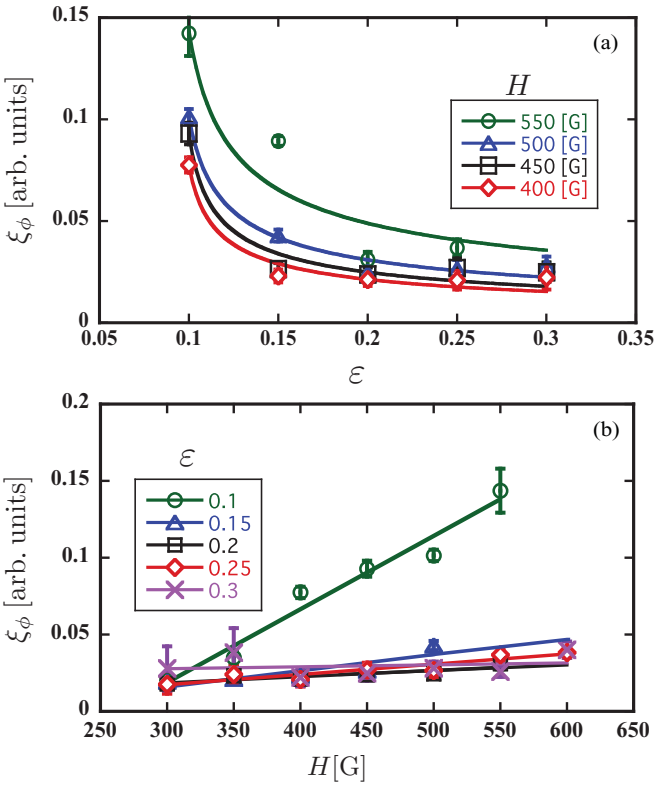

FIG. 6. (Color online) (a) ε dependence of ξ_ϕ for fixed $H = 400$ G (red diamonds), $H = 450$ G (black rectangles), $H = 500$ G (blue triangles), and $H = 550$ G (green circles), while the solid lines indicate $\xi_\phi \propto \varepsilon^{-1/2}$. (b) H dependence of ξ_ϕ for selected values of ε, the ξ_ϕ profiles scaled into two different lines. See text for details.

of a contribution the Nambu-Goldstone mode makes to the convective patterns, for example, a full contribution for $S = 0$ and no contribution for $S = 1$.

Additionally, since S is obtained directly from the 2D spectra, it is worth considering the H and ε dependence of the azimuthal peak width ω_ϕ of the 2D spectra, which correspond to the inverse of the correlation length ξ_ϕ of the pattern [23]. For SMT (also for STC A), the ε dependence of ξ_ϕ was previously reported (see Refs. [25,26]). Here we will only consider the ε dependence of ξ_ϕ for STC B. In order to obtain ω_ϕ, we fit I of the first-mode spectrum as a function of ϕ with the Lorenzian function (see Fig. 2).

Figure 6 shows the H and ε dependence of ξ_ϕ. As shown in Fig. 6(a), we observed a nontrivial ε dependence of ξ_ϕ, that is, $\xi_\phi \propto \varepsilon^{-1/2}$. Such divergent behavior of ξ_ϕ with power $-1/2$ on azimuthal angle of rolls was also observed in a rotating Rayleigh-Bénard convection, in which a Küppers-Lortz (KL) instability occurred above the critical temperature difference $\Delta T_c(\Omega_c)$ between the bottom and the top of a cell, where Ω_c is the critical dimensionless rotation rate [27]. Both SMT and KL instability in the rotating Rayleigh-Bénard convection produce STC above the onsets via a single supercritical bifurcation caused by the weak nonlinearity [20,27]. For this reason, both are of special interest, although their mechanisms are different because there is no Nambu-Goldstone mode in the KL instability.

Figure 6(b) shows the linear relationship between ξ_ϕ and H, indicating the response of $\mathbf{c}(\mathbf{r})$ to $\mathbf{H}$. Note that $\mathbf{q}(\mathbf{r})$ originated from $\mathbf{c}(\mathbf{r})$ [8]. Therefore $\mathbf{H}$, in this manner, acts as an indirect force to the orientation of $\mathbf{q}(\mathbf{r})$. As shown in Fig. 6(b) the profiles of ξ_ϕ scaled in to two different lines. For small ε ($\varepsilon < 0.15$), the response of $\mathbf{q}(\mathbf{r})$ to H was sensitive, and the profile of ξ_ϕ steeply increased with respect to H. On the other hand, the $\mathbf{q}(\mathbf{r})$ response to H was less sensitive for large ε ($\varepsilon \geqslant 0.15$), because the higher ε exerted more uncompensated torque on $\mathbf{q}(\mathbf{r})$. These results are consistent with the two different profiles of S, as explained above.

III. SUMMARY

We investigated the increase in pattern regularity of electroconvective patterns under the influence of an external magnetic field. We defined S, an improved order parameter for the convective patterns that is easily obtained from 2D spectra of the patterns. The value of S is directly related to the degrees of free rotation of the local wave vector $\mathbf{q}(\mathbf{r})$. S can also be used as a quantitative measure of the degree of pattern regularity and the extent of contribution from the Nambu-Goldstone modes. Hence, the degree of regularity of the patterns in SMT under the influence of H can be measured using S. We successfully classified two types of spatiotemporal chaos, STC A ($0 < S \leqslant 0.1$ with the plateau at $S \approx 0.1$ in the present study) and STC B ($S > 0.1$ in the present study). The transition between two ordered patterns; an abnormal zigzag pattern (Z-II) and a normal zigzag pattern (Z-I), was also clarified. The possible schematic phase diagram of patterns in the H-ε plane was proposed.

ACKNOWLEDGMENTS

This work was partially supported by Grants-in-Aid for Scientific Research (Nos. 20111003, 21340110, and 21540391) from the Ministry of Education, Culture, Sports, Science, and Technology of Japan and the Japan Society for the Promotion of Science (JSPS). R.A. acknowledges support from a Grant-in-Aid for Scientific Research (No. 20.08333) from JSPS. F.N. acknowledges support from the Directorate General of Higher Education (DIKTI), Department of National Education of Indonesia (DIKNAS). Fruitful discussions with Dr. M. Suzuki and Dr. T. Narumi are greatly appreciated.

[1] M. C. Cross and P. C. Hohenberg, Rev. Mod. Phys. **65**, 851 (1993).
[2] S. W. Morris, E. Bodenschatz, D. S. Cannell, and G. Ahlers, Phys. Rev. Lett. **71**, 2026 (1993).
[3] Y. L. Klimontovich, BioSystems **42**, 85 (1997); W. H. Sulis and I. N. Tromimova, *Non Linear Dynamics in the Life and Social Sciences* (IOS Press, Moscow, 2000).
[4] J.-H. Huh and S. Kai, Phys. Rev. E **68**, 042702 (2003).
[5] J.-H. Huh, Y. Hidaka, and S. Kai, Phys. Rev. E **58**, 7355 (1998).
[6] J.-H. Huh, Y. Hidaka, A. G. Rossberg, and S. Kai, Phys. Rev. E **61**, 2769 (2000).
[7] A. G. Rossberg, N. Éber, Á. Buka, and L. Kramer, Phys. Rev. E **61**, R25 (2000).
[8] Y. Hidaka, K. Tamura, and S. Kai, Prog. Theor. Phys. Suppl. **161**, 1 (2006).
[9] A. Hertrich, W. Decker, W. Pesch, and L. Kramer, J. Phys. II (France) **2**, 1915 (1992).
[10] M. I. Tribelsky and K. Tsuboi, Phys. Rev. Lett. **76**, 1631 (1996).
[11] H. Richter, N. Klöpper, A. Hertrich, and Á. Buka, Europhys. Lett. **30**, 37 (1995).
[12] S. Kai, K. Hayashi, and Y. Hidaka, J. Phys. Chem. **100**, 19007 (1996).
[13] A. G. Rossberg, Ph.D. thesis, University of Bayreuth, 1998.
[14] W. Zimmermann and L. Kramer, Phys. Rev. Lett. **55**, 402 (1985).
[15] J.-H. Huh, Y. Hidaka, and S. Kai, J. Phys. Soc. Jpn. **68**, 1567 (1999).
[16] E. Bodenschatz, W. Zimmermann, and L. Kramer, J. Phys. France **49**, 1875 (1988).
[17] F. Nugroho, T. Ueki, R. Anugraha, Y. Hidaka, and S. Kai, J. Phys. Soc. Jpn. **79**, 123001 (2010).
[18] P. Tóth, Á. Buka, J. Peinke, and L. Kramer, Phys. Rev. E **58**, 1983 (1998).
[19] A. G. Rossberg and L. Kramer, Phys. Scr. T **67**, 121 (1996).
[20] A. G. Rossberg, A. Hertrich, L. Kramer, and W. Pesch, Phys. Rev. Lett. **76**, 4729 (1996).
[21] J.-H. Huh, Y. Hidaka, and S. Kai, J. Phys. Soc. Jpn. **67**, 1948 (1998).
[22] N. Éber, S. Németh, A. G. Rossberg, L. Kramer, and A. Buka, Phys. Rev. E **66**, 036213 (2002).
[23] R. Anugraha, Y. Hidaka, N. Oikawa, and S. Kai, J. Phys. Soc. Jpn. **77**, 073001 (2008).
[24] It is well known in the far from equilibrium system that the relative degree of chaos, coined as *norm of chaos* in Ref. [3], can be measured from how much the systems deviates from an order state and vice versa.
[25] K. Tamura, Y. Hidaka, Y. Yusuf, and S. Kai, Physica A **306**, 157 (2002).
[26] K. Tamura, R. Anugraha, R. Matsuo, Y. Hidaka, N. Oikawa, and S. Kai, J. Phys. Soc. Jpn. **75**, 063801 (2006).
[27] Y. Hu, W. Pesch, G. Ahlers, and R. E. Ecke, Phys. Rev. E **58**, 5821 (1998).